nzsee
NEW ZEALAND SOCIETY FOR EARTHQUAKE ENGINEERING

Insights from the 2021 New Zealand Strong Ground Motion Database

J.A. Hutchinson, Brendon Bradley, Robin Lee, Claudio Schill, Mike Dupuis & Jason Motha
University of Canterbury, Christchurch, Christchurch, New Zealand

Chris van Houtte, Anna Kaiser & Elena Manea
GNS Science, Lower Hutt, New Zealand

Liam Wotherspoon
The University of Auckland, Auckland, New Zealand.

ABSTRACT

New Zealand has a wide variety of tectonic settings and environments, which experience earthquakes to varying degrees of severity. The shaking experienced by an earthquake is quantified by strong ground motion intensity measures, which must be computed and collated into a consistent catalogue. We present information regarding the development and implementation of the 2021 New Zealand strong ground motion database. Strong motion intensity measures have been computed for events with magnitudes equal to or greater than 4 from 2000 through the end of 2021. Along with these intensity measures, we have determined earthquake rupture properties, recomputed earthquake magnitudes, determined event tectonic classifications, and derived source-receiver propagation path information. This information is compiled in several tables, which comprise the entire database. This database establishes a unified, expandable catalogue necessary for implementation with hazard modelling studies for a wide variety of regions across New Zealand.

1 INTRODUCTION

New Zealand (NZ) is a tectonically diverse country with opposing subduction zones beneath the northern and southern islands that are joined by the nearly 500 km long right-lateral Alpine fault. For nearly two decades, continuous records of earthquakes have been recorded, located, and catalogued in NZ with the GeoNet project. These records can be easily accessed and downloaded via an FDSN webservice with popular tools such as the ObsPy module (Krischer et al., 2015; Wassermann et al., 2010) for the Python programming language. The information for hundreds of thousands of events can be accessed using the GeoNet Quake Search tool: https://quakesearch.geonet.org.nz.

While the majority of earthquakes have small magnitudes (< 4), there have been several large and devastating ruptures since 2010. These include the 2010 M 7.2 Darfield, 2011 M 6.2 Christchurch, and 2016 M 7.8 Kaikōura events. The 22 February 2011 M 6.2 Christchurch earthquake was responsible for at the least an estimated NZ$40 billion in damages to Christchurch city (Noy et al., 2016), and was itself an aftershock of the M 7.2 Darfield earthquake, which occurred on 3 September, 2010. The aftershock sequence of the 2010-2011 Canterbury earthquakes led to the discovery a previously unmapped fault system (as was the Darfield rupture), extending to a depth of approximately 10 km (Bannister et al., 2011). Significant aftershocks proceeded with the 13 June 2011 Mw 6.0 and 23 December 2011 Mw 5.9 Christchurch earthquakes. An examination of these events and other significant earthquakes have informed the drive behind developing seismic hazard models based on ground-motion predictions, fault distributions, and site characteristics (e.g. Bradley, 2019; Dempsey et al., 2020; de la Torre et al., 2020). To further inform and improve on these models, a robust strong ground motion database is essential. For example, the data from this project will contribute towards the upcoming 2022 National Seismic Hazard Model (NSHM) update.

This article describes the implementation of procedures for developing the New Zealand strong motion database. The aim of the database is to provide a central resource for analysts and modellers to utilize in developing seismic hazard models for New Zealand's geologically diverse settings. Following the initial full release (v. 1.0), we have already updated the database to include strong motion intensity measures through 2021. Regular updates are planned to maintain and expand the database beyond 2021.

2 OVERVIEW OF THE DATABASE

The 2021 New Zealand (NZ) strong ground motion database ("the Database") is comprised of multiple tables that collectively define strong-motion intensity measure data and underlying metadata associated with earthquake rupture, path, site effects and instrument properties. Specifically, these tables are organised in a relational database, depicted in Figure 1, which include tables for earthquake source, site, propagation path, station magnitude, phase arrival, and ground-motion intensity measure (IM) data. The constituent data within the relational database include compiled data from numerous references and databases, and new data computed as part of this project. The completed database can be retrieved online from https://osf.io/q9yrg/?view_only=05337ba1ebc744fc96b9924de633ca0e. A complete description of the fields within each table are given in the Wiki for the provided link, along with a version history.

Presently, the Database is complete for high-quality ground motions (defined subsequently) from earthquakes with magnitudes ≥ 4 from the GeoNet network over the period 1 January 2000 through 31 December 2021. The Database comprises 12,725 earthquakes of multiple tectonic types, as shown in Figure 2. The (moment) magnitude vs. source-to-site distance (R_{rup}) distribution of the 196,044 ground motions recorded at 543 different seismic instrument locations is shown in Figure 3.

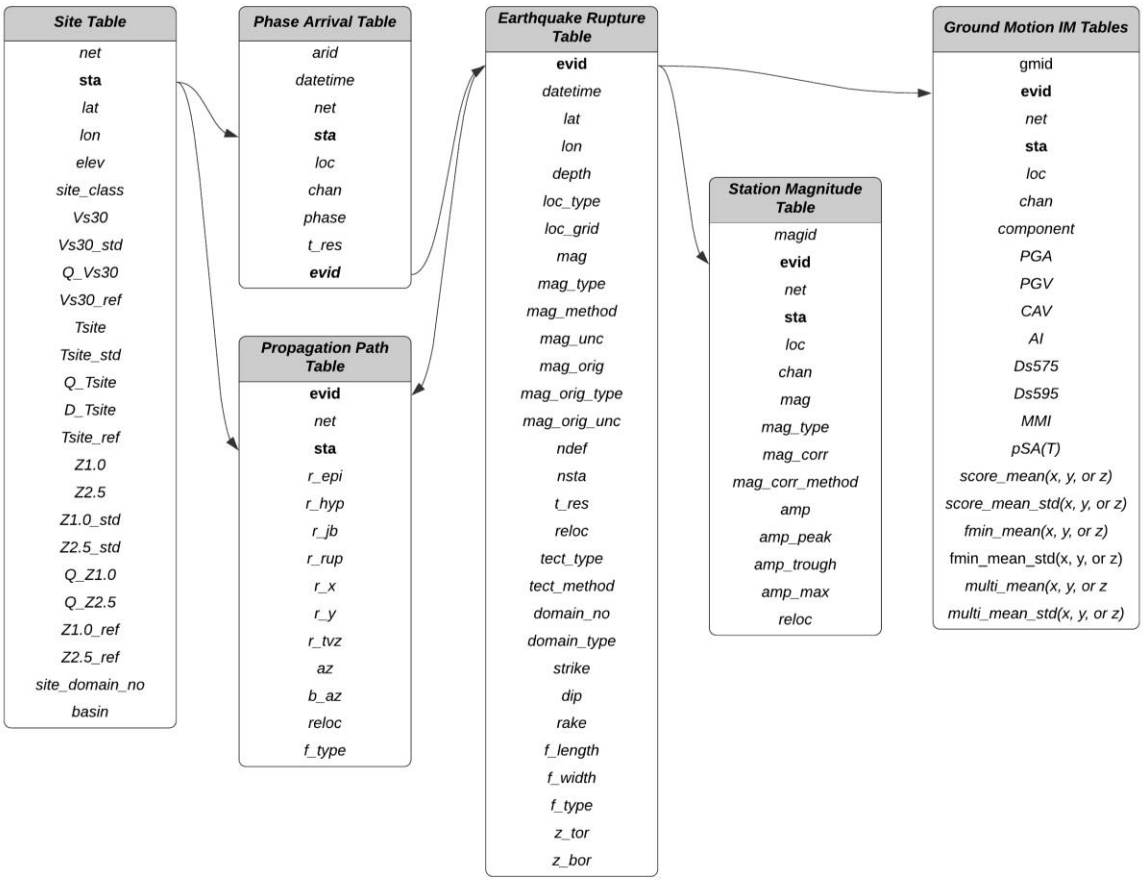

Figure 1. Schematic of the relational setting of six tables within the NZ Strong Motion Database. Bold terms indicate properties that provide relational connectivity between the different tables.

The development of this Database has two primary objectives. Firstly, to significantly expand on the number of ground motions, events, and dataset quality from the previous NZ Strong Motion Database (NZSMDB; Van Houtte et al., 2017). Secondly, to provide a NZ-specific observational dataset that can be used for the examination of the predictive performance of existing empirical ground-motion models, as well as the development of new ground-motion models (either from scratch, or adjustments to existing models) – both empirical and simulation-based in nature. In comparison to the previous NZ strong motion database by Van Houtte et al. (2017), we expand the number of events with records by a factor of ~45 and the number of three-component seismograms by a factor of ~50.

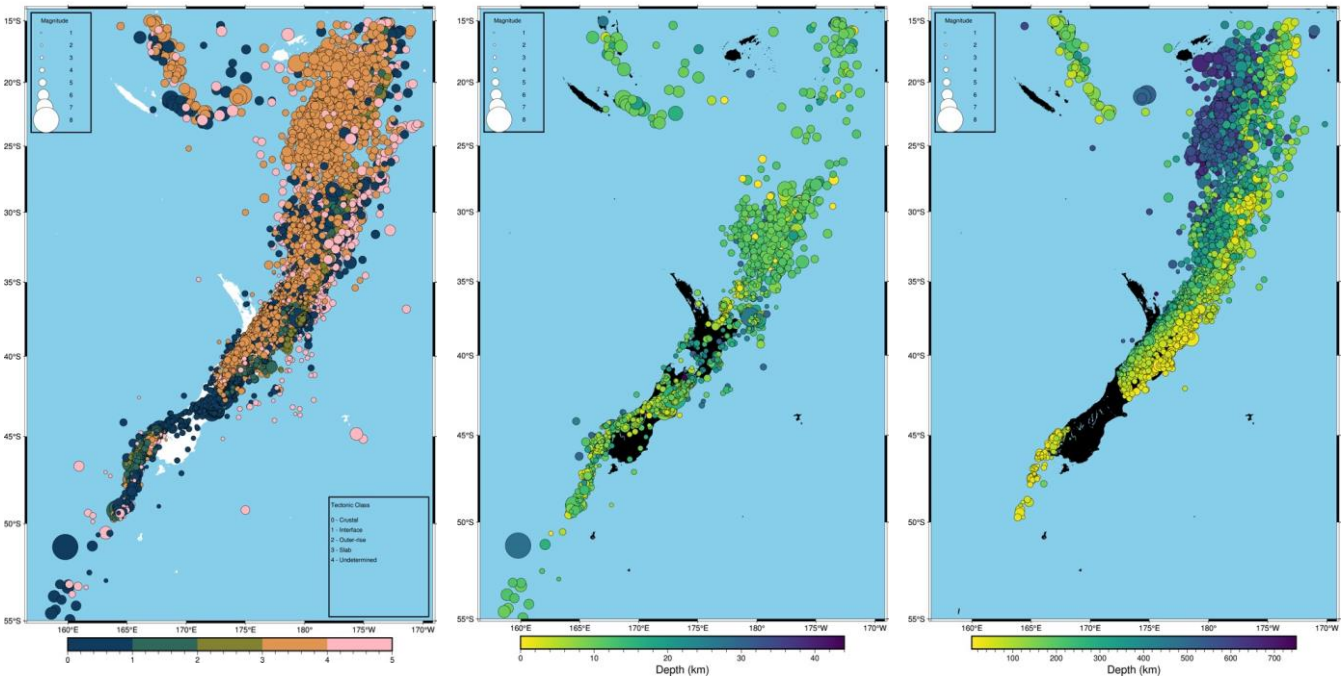

Figure 2. a) Geographical distribution of all events by tectonic type. b) Distribution of crustal earthquakes by depth. c) Distribution of slab earthquakes by depth.

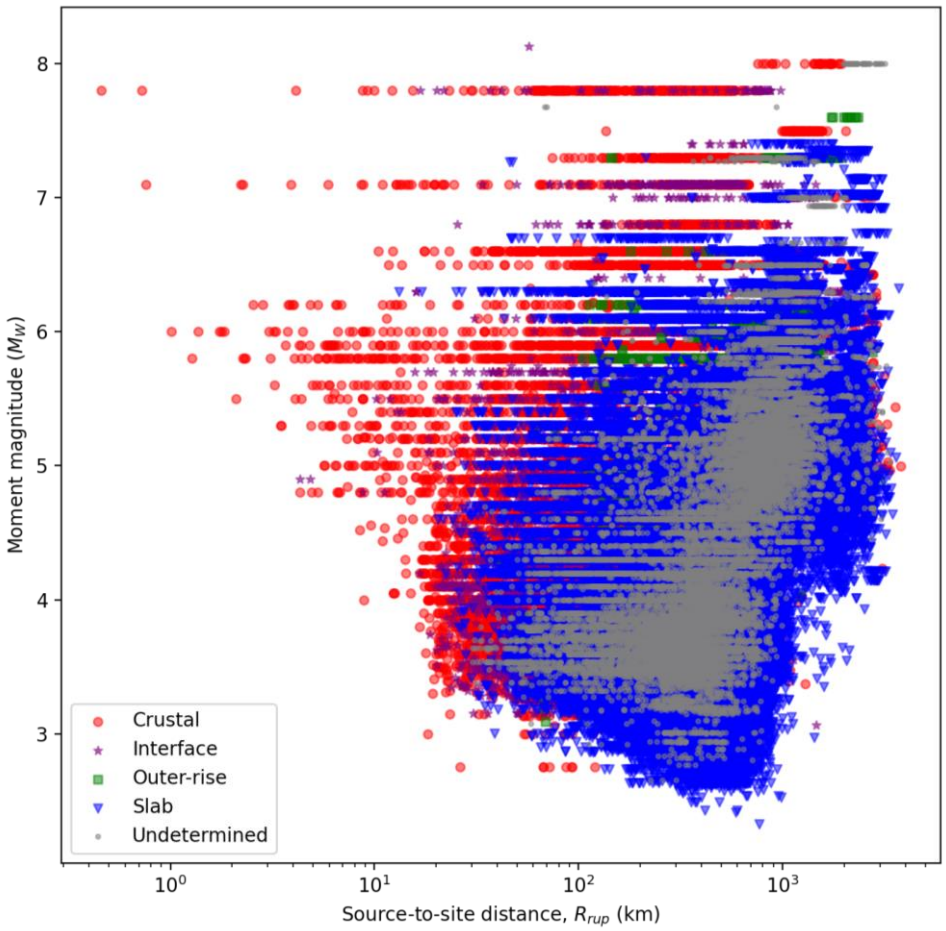

Figure 3. Magnitude-distance distribution of the ground-motions in the Database.

3 METHODS USED FOR DEVELOPING THE DATABASE

Much of the information provided in the Database is computed from the relational dependencies of multiple sources. For example, if fault plane metrics are unknown, calculating the source to site distance R_{rup} requires a hypocentre, earthquake magnitude, and earthquake rupture properties (strike, dip, and rake). All of these parameters must be consistently implemented for direct comparisons amongst events. We outline several of the most important procedures implemented for the development of the Database in the following sections.

3.1 Earthquake locations

The Database ultimately requires rupture geometries and subsequently source-to-site distance metrics. For many earthquakes (particularly those of small-to-moderate magnitude), such information is derived from earthquake hypocentral locations that are provided as latitude, longitude, and depth coordinates. Unless otherwise indicated by the *reloc* field, the location of these events originates from the GeoNet database.

For a subset of the Database event locations, earthquake hypocentres have been previously relocated (Reyners et al., 2011). A total of over 100,000 relocations were computed for events that occurred from 2001 January – 2010 March. Of these events, approximately 2000 are included in the Database and are indicated by the 'relocated' column in several of the tables.

Figure 4 shows the Euclidian location difference between original and relocated hypocenter locations in the Database. The mean and standard deviation differences are 19.8 and 38.8 km, respectively. The size of the location differences illustrates that a substantial area for further improvement is to significantly increase the proportion of events in the Database which have been relocated.

Local magnitude values in the Reyners et al. (2011) relocated catalogue were not recalculated and are identical to the values from the original GeoNet hypocenters. For this database, the local relocated event magnitudes have been corrected with the method described subsequently in Section 3.2.

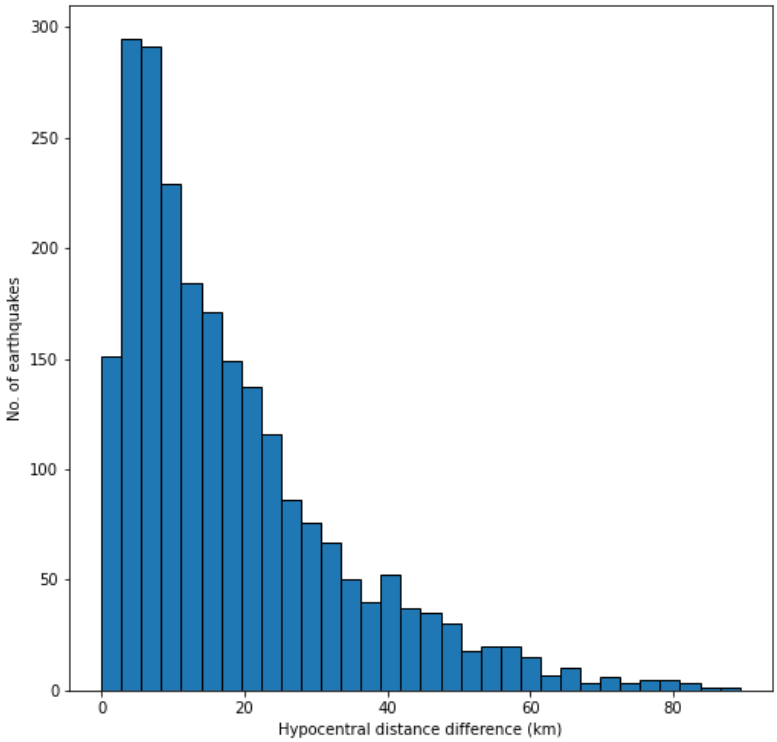

Figure 4. Frequency of difference in distance from original hypocenters as reported by GeoNet to relocated hypocenters.

3.2 Earthquake magnitude estimates

Harmonization of magnitude estimates requires the determination of moment magnitudes for all events in the Database. Since 2003, manual calculation of moment tensor solutions for moderate-to-large magnitude earthquakes have been undertaken (Herrmann, 2013; Ristau, 2013), with a total of 1,929 events from moment magnitude 3.4 to 8.0 in the Database.

The majority of remaining events have local magnitude (M_L) estimates that are retrieved from the GeoNet database. These magnitudes are corrected with the equations of Rhoades et al. (2020) to more closely represent the true moment magnitude (M_W) unless waveform and/or instrument response information is unavailable.

In order to recalculate magnitude for each station where a phase arrival was detected, we attempt to retrieve instrument response and waveform data. It should be noted that instrument response and/or waveform data is not always available, especially for events in the early 2000s. For all available channels (horizontal and vertical), we calculate the peak displacement amplitude (in mm) of the body waves after correcting the seismogram to the Wood-Anderson response. For waveforms with a signal-to-noise ratio >= 3, the amplitude is used as input to compute the local station magnitude. Typically, we prefer magnitudes on the vertical channel, however, the mean of the two horizontal components is used when vertical data is corrupt or otherwise unavailable. Finally, the mean of the local station magnitudes, excluding outliers, is used to determine the corrected local magnitude (cM_L).

The bulk of events (~5,500) have been magnitude corrected, while M_W and M_B measures comprise most of the remaining data. In some cases, M_L measures could not be corrected, due to a lack of available waveform data. For these values, a scaling relationship derived from Rhoades et al. (2020) can be used, however such a relationship cannot be applied to relocated hypocentres. The magnitude distribution of cM_L data is shown in Figure 5.

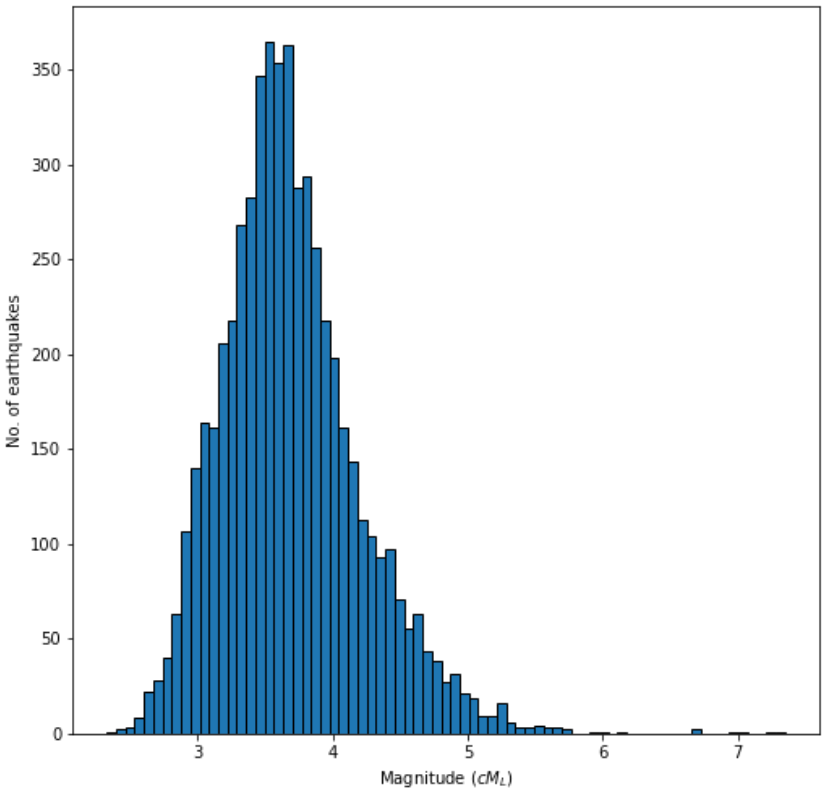

Figure 5. Magnitude distribution of corrected local magnitudes (cM_L).

3.3 Tectonic classification

The tectonic classification of an event is determined based on the location of the event relative to various subduction geometry models. Possible classifications include crustal, slab, interface, outer rise, and undetermined.

For the method used to determine tectonic classifications, results from Van Houtte et al. (2017), are preferred. For events not included in Van Houtte et al. (2017), we utilize the blended slab models of Hayes et al. (2018) and Williams et al. (2013) for an optimal geometry (Charles Williams via Chris Rollins, personal comm., 2021).

The number of observed earthquakes by tectonic type is shown in Figure 6 and the spatial distribution of these events is shown in Figure 2a. The majority of events are considered either crustal or slab earthquakes. Crustal earthquakes span across the entirety of NZ and are predominant along the Alpine Fault and into Fiordland to the southwest. Slab earthquakes are most abundant beneath the North Island and to the northeast within the subducting Pacific plate.

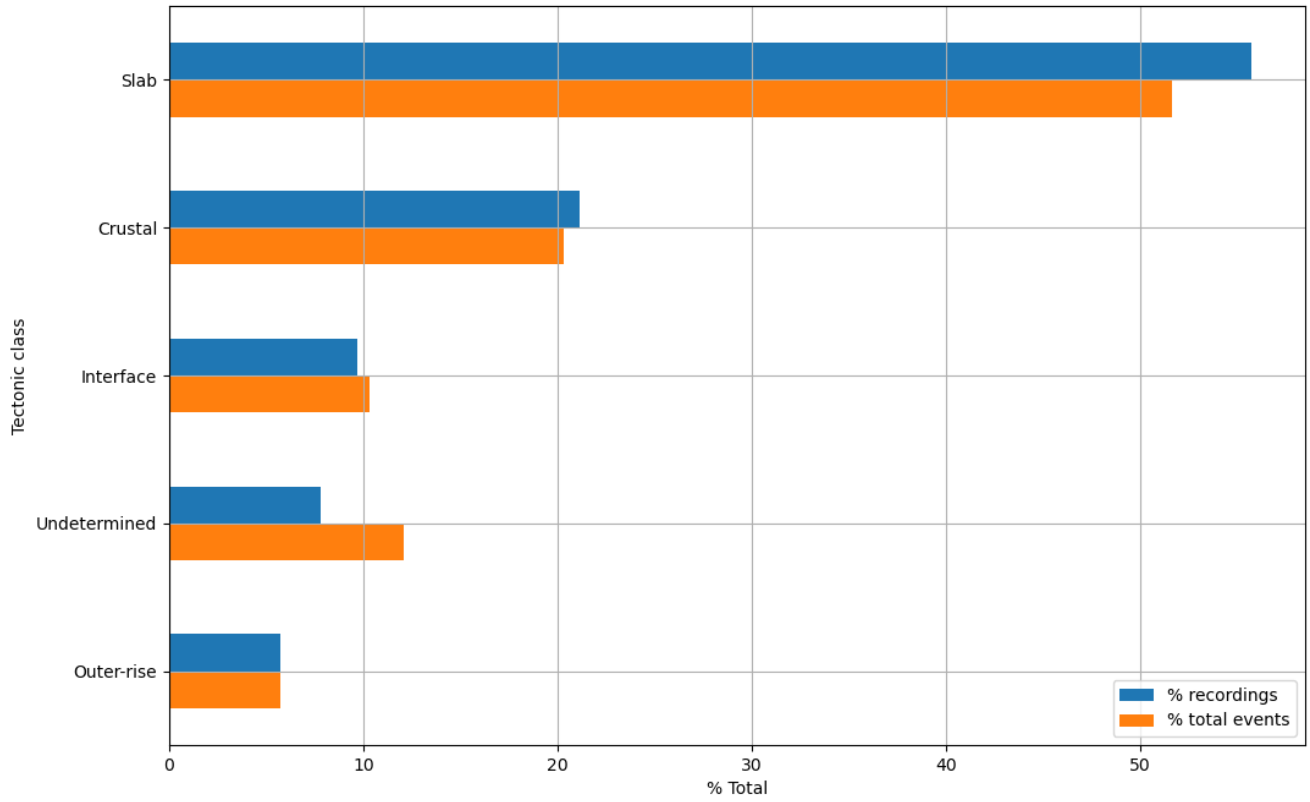

Figure 6. Percentage of records (blue) and events (orange) by tectonic class.

3.4 Neotectonic domain regionalization earthquake rupture characteristics

The domain number of an earthquake corresponds to one of 28 neotectonic domains in NZ in which it occurred (Rattenbury, 2021). These domains are classified based on the dominant fault type (strike-slip, extensional|normal, or contractional|reverse), which is listed as the domain type, and are used to determine the general fault properties of encompassed earthquakes. Any events outside of the listed tectonic domains are considered contractional.

The strike, dip, and rake of an event is determined via a prioritized system from available resources. Starting from highest priority, we first choose strike, dip, and rake from finite-fault data. Currently, the Database uses

finite fault geometries for three events; the M_W 7.2 2010 Darfield earthquake, the M_W 6.2 2011 Christchurch earthquake, and the M_W 7.8 Kaikōura earthquake. If finite-fault data are unavailable, centroid moment tensor (CMT) solutions that have been hand-reviewed are used to determine the most likely fault plane (personal comm., Lee, 2021). Other CMT solutions are compared with their neotectonic domain to find the nearest strike to determine the preferred fault plane. Finally, if none of the above are available, we use average fault orientations from the 28 tectonic domains to determine strike, dip, and rake. Any events located outside of the tectonic domains are considered contractional and are assigned a standard strike, dip, and rake of 220/45/090 degrees.

If finite fault geometry is unavailable for an earthquake, along-strike length (f_length), down-dip width (f_width or W), depth to the top of the rupture (z_tor), and depth to the bottom of the rupture (z_bor), must be computed in order to determine the fault geometry for source – receiver propagation path information.

Along-strike length and the down-dip distance are computed based on the magnitude-scaling relationships of Leonard (2014) and Skarlatoudis et al. (2016) for crustal and subduction events, respectively. The depth to the top of the rupture is determined by subtracting half of the rupture height from the fault depth, while Z_{BOR} is simply the height of the fault in addition to Z_{TOR}. In cases where Z_{TOR} would be reported as a negative depth, it is corrected to a value of 0, with the Z_{BOR} value adjusted such that the correct down-dip width is maintained.

3.5 Site data prioritization

Vs30, T site, and Z1.0/Z2.5 site data are drawn from several sources. Data are prioritized based on quality (Q) and the source references are reported in the *ref* category for each measure. The frequency of stations is compared to the Vs30 values in Figure 7a, which shows histograms for both measure and inferred Vs30 data. Further, the frequency of stations is compared to the Z1.0 data for Q1 and Q2/Q3 measures in Figure 7b, and Vs30 vs Z1.0 values are shown in Figure 7c, with colour indicating the underlying basin for each site.

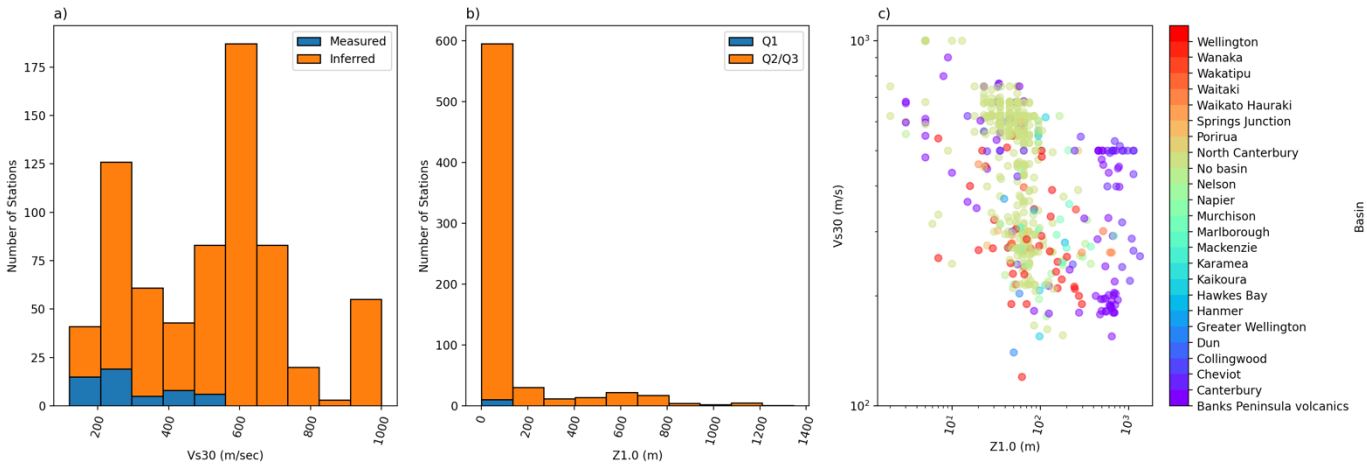

Figure 7. a) Frequency of stations by Vs30 values in meters/sec. b) Frequency of stations by Z1.0 values in meters. c) Z1.0 values vs Vs30 values with colour indicating the underlying basin.

3.6 Source-to-site distance metrics

From the fault geometries, source-to-site distance metrics can be determined. The propagation path table includes seven different measures. R_{epi} and R_{hyp} are the epicentral and hypocentral distances (in km) from the event to the instrument station. Both R_{jb} and R_{rup} depend on the fault properties of the event, further discussed in Section 3.4. R_{jb} is the shortest distance (in km) measured to the surface projection of the event

rupture plane. R_{rup} is the shortest distance (in km) to the rupture plane. For small magnitude events, R_{jb} and R_{rup} are roughly equivalent to R_{epi} and R_{hyp}, respectively. R_x and R_y are measured perpendicular and parallel the fault strike of the event, respectively, and are distances (in km) from the central point of the surface projection of the up-dip edge of the fault plane. R_{tvz} is the decimal fraction of R_{epi} which travelled through the Taupō Volcanic Zone (TVZ).

3.7 Strong ground-motion intensity measures

Waveform records are selected for extraction and classification based on several factors:

1) The event magnitude as reported by GeoNet must be equal to or exceed the magnitude threshold (currently M 4).
2) Station metadata (latitude, longitude, and elevation) is available for the recording instrument.
3) If a station has multiple recording instruments, high sample-rate accelerometers are preferred (HN), followed by lower sample-rate accelerometers (BN), high sample-rate broadband seismometers (HH), lower sample-rate broadband seismometers (BH), extremely short-period seismometers (EH), and finally short period seismometers (SH).
4) Instrument response for the given instrument and time period must be available, otherwise the waveform will be rejected.
5) Data is rotated to ZNE components if it is in Z12 components.

The quality of the data is assessed with a ground-motion classifier, GMC (Dupuis et al., 2022). GMC is a deep-learning-based model specifically developed for predicting the quality of ground-motions in NZ on a scale of 0 – 1. Classification is performed independently for all three components of the seismogram. For the Database, quality scores ≥ 0.5 are considered of a high enough quality for IM computations.

Ims are computed for 000 (N), 090 (E), and vertical (Z) components, as well as the average horizontal (RotD50) and maximum horizontal (RotD50) pseudo-acceleration spectra (pSAs). Further IMs in include PGA (peak ground acceleration), PGV (peak ground velocity), CAV (cumulative absolute velocity), AI (Arias intensity), Ds_{575} (5-75% significant duration), Ds_{595} (5-95% significant duration), and MMI (modified Mercalli intensity).

From 2000 – 2021, the number of IMs gradually increases (Figure 8). This increase in records coincides with the availability of waveform data and the addition of new stations to the NZ network. 2016 contains an anomalously high number of records due to the Kaikōura aftershock sequence. Similarly, for 2021 a large number of aftershocks were produced by the M 7.3 East Cape earthquake and the M 7.4 and M 8.1 Kermadec earthquakes, all of which occurred on 5 March (NZDT), 2021.

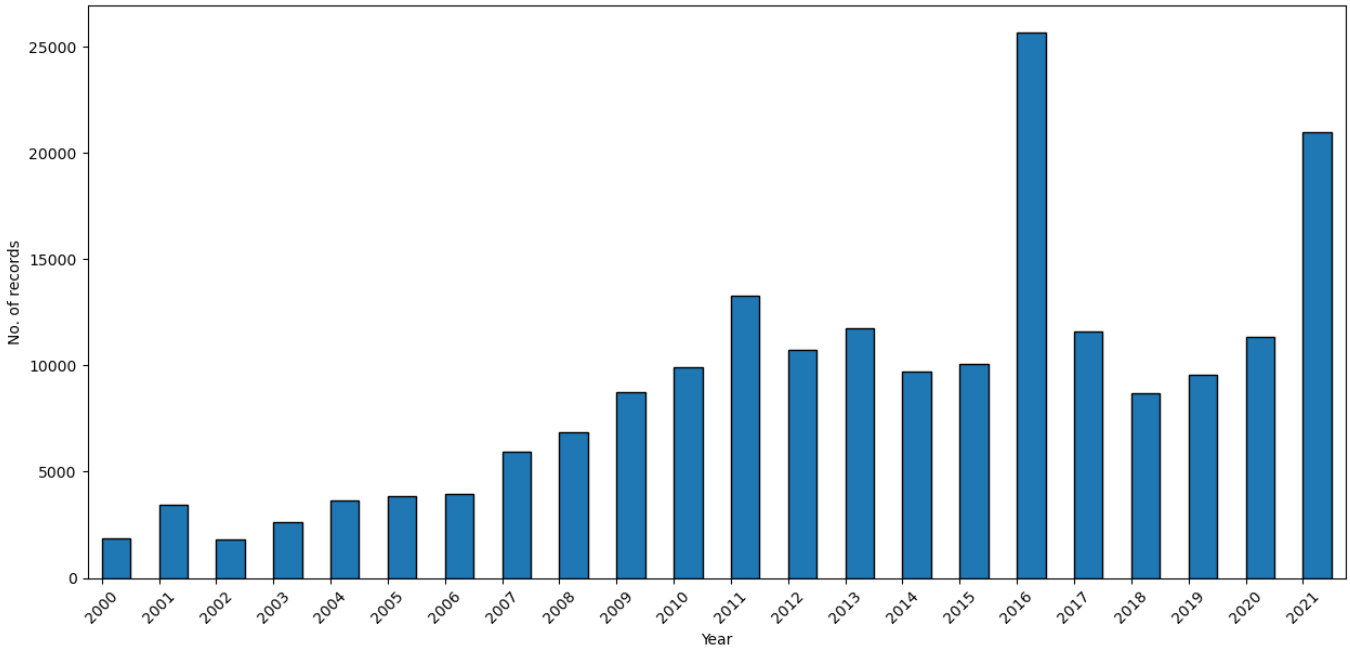

Figure 8. Number of RotD50 records by year.

4 CONCLUSIONS

The first version (v1.0) of the NZ strong ground-motion database provides a complete record of intensity measures for all events from the GeoNet database with a magnitude equal to or greater than 4 from the year 2000 until 31 December 2021. Among many possibilities, these data can be utilized for developing ground-motion hazard models, assessing site conditions, and investigating attenuation.

The Database has been developed with continuous updates in mind, expanding the date and magnitude range as further processing is performed. In addition, the modular nature of the Database allows for the implementation of further data, such as focal mechanism solutions and hypocentre relocations. Finally, we intend to update the data with the latest information from other sources, such as site information in the site table and recomputed intensity measures for recalibrated instruments, in order to maintain an accurate and reliable catalogue.

5 REFERENCES

Bannister, S., Fry, B., Reyners, M., Ristau, J., and Zhang, H. (2011). Fine-scale relocation of aftershocks of the 22 February Mw 6.2 Christchurch earthquake using double-difference tomography. *Seismological Research Letters*, *82*(6), 839–845. https://doi.org/10.1785/gssrl.82.6.839

Bradley, B. A. (2019). On-going challenges in physics-based ground motion prediction and insights from the 2010–2011 Canterbury and 2016 Kaikoura, New Zealand earthquakes. *Soil Dynamics and Earthquake Engineering*, *124*, 354–364. https://doi.org/10.1016/j.soildyn.2018.04.042

Dempsey, D., Eccles, J. D., Huang, J., Jeong, S., Nicolin, E., Stolte, A., Wotherspoon, L., and Bradley, B. A. (2020). Ground motion simulation of hypothetical earthquakes in the upper North Island of New Zealand. *New Zealand Journal of Geology and Geophysics*. https://doi.org/10.1080/00288306.2020.1842469

Dupuis, M., Schill, C., Lee, R., and Bradley, B. (2022). A deep-learning-based model for quality assessment of earthquake-induced ground-motion records. *[Unpublished Manuscript]*.

Hayes, G. P., Moore, G. L., Portner, D. E., Hearne, M., Flamme, H., Furtney, M., and Smoczyk, G. M.

(2018). Slab2, a comprehensive subduction zone geometry model. *Science*, *362*(6410), 58–61. https://doi.org/10.1126/science.aat4723

Herrmann, R. B. (2013). Computer programs in seismology: An evolving tool for instruction and research. *Seismological Research Letters*, *84*(6), 1081–1088. https://doi.org/10.1785/0220110096

Van Houtte, C., Bannister, S., Holden, C., Bourguignon, S., and Mcverry, G. (2017). The New Zealand strong motion database. *Bulletin of the New Zealand Society for Earthquake Engineering*, *50*(1), 1–20. https://doi.org/10.5459/bnzsee.50.1.1-20

Krischer, L., Megies, T., Barsch, R., Beyreuther, M., Lecocq, T., Caudron, C., and Wassermann, J. (2015). ObsPy: a bridge for seismology into the scientific Python ecosystem. *Computational Science & Discovery*, *8*(1), 014003. https://doi.org/10.1088/1749-4699/8/1/014003

de la Torre, C. A., Bradley, B. A., and Lee, R. L. (2020). Modeling nonlinear site effects in physics-based ground motion simulations of the 2010–2011 Canterbury earthquake sequence. *Earthquake Spectra*, *36*(2), 856–879. https://doi.org/10.1177/8755293019891729

Leonard, M. (2014). Self-consistent earthquake fault-scaling relations: Update and extension to stable continental strike-slip faults. *Bulletin of the Seismological Society of America*, *104*(6), 2953–2965. https://doi.org/10.1785/0120140087

Noy, I., Parker, M., and Wood, A. (2016). The Canterbury rebuild five years on from the Christchurch earthquake. *Reserve Bank of New Zealand Bulletin*, *79*(3), 3. Retrieved from https://www.questia.com/library/journal/1G1-452290686/the-canterbury-rebuild-five-years-on-from-the-christchurch

Rattenbury, M. (2021). *Regional fault data orientation and length analysis to potentially inform on distributed seismicity for the National Seismic Hazard Model revision project*.

Reyners, M., Eberhart-Phillips, D., and Bannister, S. (2011). Tracking repeated subduction of the Hikurangi Plateau beneath New Zealand. *Earth and Planetary Science Letters*, *311*(1–2), 165–171. https://doi.org/10.1016/j.epsl.2011.09.011

Rhoades, D. A., Christophersen, A., Bourguignon, S., Ristau, J., and Salichon, J. (2020). A Depth-Dependent Local Magnitude Scale for New Zealand Earthquakes Consistent with Moment Magnitude. *Bulletin of the Seismological Society of America*. https://doi.org/10.1785/0120200252

Ristau, J. (2013). Update of regional moment tensor analysis for earthquakes in New Zealand and adjacent offshore regions. *Bulletin of the Seismological Society of America*, *103*(4), 2520–2533. https://doi.org/10.1785/0120120339

Skarlatoudis, A. A., Somerville, P. G., and Thio, H. K. (2016). Source-scaling relations of interface subduction earthquakes for strong ground motion and tsunami simulation. *Bulletin of the Seismological Society of America*, *106*(4), 1652–1662. https://doi.org/10.1785/0120150320

Wassermann, J., Barsch, R., Beyreuther, M., Behr, Y., Megies, T., and Krischer, L. (2010). ObsPy: A Python Toolbox for Seismology. *Seismological Research Letters*, *81*(3), 530–533. https://doi.org/10.1785/gssrl.81.3.530

Williams, C. A., Eberhart-Phillips, D., Bannister, S., Barker, D. H. N., Henrys, S., Reyners, M., and Sutherland, R. (2013). Revised interface geometry for the hikurangi subduction zone, New Zealand. *Seismological Research Letters*, *84*(6), 1066–1073. https://doi.org/10.1785/0220130035